

Short Papers

The Q -Factor of Coaxial Resonators Partially Loaded with High Dielectric Constant Microwave Ceramics

SADAHICO YAMASHITA, MEMBER, IEEE, AND MITSUO MAKIMOTO

Abstract — The quality factor of partially loaded dielectric coaxial stepped impedance resonators (PDSIR) has been analyzed, including analysis of the dielectric constant ϵ_r and the dielectric loss $\tan \delta$ of the ceramics. The Q -factor of several resonators is also calculated and compared with the experimental results. This shows that the Q -factor degradation lessens even though the resonator length becomes small when the total length $L_t > 1/\sqrt{\epsilon_r}$, and becomes large when $L_t < 1/\sqrt{\epsilon_r}$.

I. INTRODUCTION

The stepped impedance resonator has been introduced and analyzed to achieve miniaturization of high Q resonators [1]. Effective reduction in size can be achieved by employing high dielectric constant ceramics for coaxial resonators. The TEM-mode coaxial resonators of fully dielectric-loaded ceramics have also been introduced [2], [3], and the authors have introduced a partially loaded dielectric ceramic stepped impedance resonator (PDSIR) to reduce resonator size.

In this paper, the Q -factor of a PDSIR is analyzed and compared with a few experimental results. To obtain a high Q -factor, it is important to use low-loss microwave ceramics and high dielectric material to make the resonator more compact. The Q -factors are calculated for a copper conductor with dielectric ceramics of dielectric constant $\epsilon_r = 35$, including the loss tangent factor of the ceramics. The experimental results are obtained at 900 MHz. The dielectric used here have a loss tangent factor of 1×10^{-4} at X-band [4].

II. THEORETICAL ANALYSIS

The PDSIR is shown in Fig. 1. The Q -factor can be obtained from the general definition which is given by

$$Q = 2\pi f_0 \cdot \frac{\text{energy stored}}{\text{energy lost per cycle}}. \quad (1)$$

The Q -factor is calculated by considering two transmission lines and using the parameters shown in Fig. 1. The current and voltage distribution in line I is considered as

$$\begin{aligned} I(x) &= I_0 \cos \beta_1 x \\ V(x) &= jZ_1 I_0 \sin \beta_1 x. \end{aligned} \quad (2)$$

At resonance, the stored energy in the form of magnetostatic energy and that of electrostatic energy are equal. The electromagnetic energy in the inductance is then considered. The unit length inductance in line I can be expressed as

$$L_1 = (\mu_0/4\pi) \ln(b/a_1) \quad (3)$$

where

$$\mu_0 = 4\pi \times 10^{-7} (H/m).$$

Manuscript received September 7, 1982; revised January 8, 1983.
The authors are with the Matsushita Research Institute Tokyo, Inc., Higashimita, Tama-ku, Kawasaki, Japan 214.

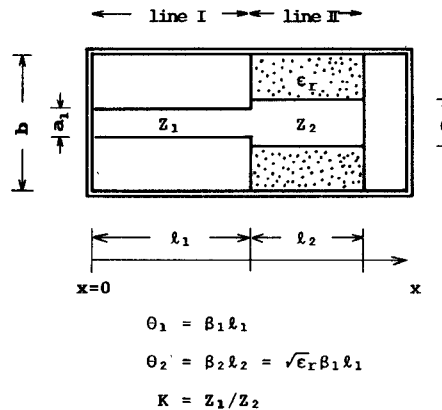


Fig. 1. Cross-sectional view of a PDSIR under analysis.

The stored energy W_1 in line I can be obtained using (2)

$$\begin{aligned} W_1 &= (L_1/2) \int_0^{l_1} |I_0(x)|^2 dx \\ &= (L_1 I_0^2/8\beta_1) (2\theta_1 + \sin 2\theta_1) \end{aligned} \quad (4)$$

where $\theta_1 = \beta_1 l_1$ and β_1 is the phase constant.

The voltage and current distribution in line II can be expressed with the condition of current continuity at $x = l_1$ from (2)

$$\begin{aligned} I(x) &= I_0 (\cos \theta_1 / \sin \theta_2) \sin \beta_2 (l_2 - x) \\ V(x) &= jV_0 \cos \beta_2 (l_2 - x) \end{aligned} \quad (5)$$

where

$$\beta_2 = \sqrt{\epsilon_r} \beta_1, \quad \theta_2 = \beta_2 l_2.$$

Then the stored energy in line II is

$$\begin{aligned} W_2 &= (L_2/2) \int_{l_1}^{l_1+l_2} |I(x)|^2 dx \\ &= (L_2 I_0^2/8\beta_2) (\cos \theta_1 / \sin \theta_2)^2 (2\theta_2 - \sin 2\theta_2) \end{aligned} \quad (6)$$

where

$$L_2 = (\mu_0/4\pi) \ln(b/a_2).$$

The lost energy is in three parts: the lost energy in the shorted end section of line I (P_s), the lost energy in line I (P_1), and that in line II (P_2). The edge capacitance effect of the open section of line II is ignored here.

The total resistance R in the shorted end section using the surface resistivity r_s can be expressed as

$$R = \int_{a_1}^b r_s / (2\pi r) dr = r_s / (2\pi) l_n (b/a_1). \quad (7)$$

Thus the lost energy is

$$P_s = (1/2) I_0^2 R = (r_s/4\pi) I_0^2 l_n (b/a_1). \quad (8)$$

The voltage and current at $x = l_1$ in line I taken from the shorted end point and at $x = l_2$ in line II taken from the open end point can be obtained from the transmission equation of each line since the current is equal at the point where the

impedance becomes stepped (see Appendix)

$$\begin{aligned} V_1 &= I_0 Z_1 (\alpha_1 l_1 \cos \theta_1 + j \sin \theta_1) \\ I_1 &= I_0 (\cos \theta_1 + j \alpha_1 l_1 \sin \theta_1) \\ V_2 &= I_0 Z_2 (\cos \theta_2 + j \alpha_2 l_2 \sin \theta_2) \\ I_2 &= I_0 (\cos \theta_2 / \sin \theta_2) (\alpha_2 l_2 \cos \theta_2 + j \sin \theta_2). \end{aligned} \quad (9)$$

Therefore, the lost energy in line I and II is as follows:

$$\begin{aligned} P_1 &= (1/2) |V_1| \cdot |I_1| \cos \theta_s \\ P_2 &= (1/2) |V_2| \cdot |I_2| \cos \theta_0 \end{aligned} \quad (10)$$

where θ_s and θ_0 represent phase difference in the voltage and current of each line.

Thus, the Q -factor can be obtained from (1)

$$Q = 2\pi f_0 \cdot \frac{W_1 + W_2}{P_s + P_1 + P_2}. \quad (11)$$

The conductor loss constant α_1 and α_2 are estimated from the expression [5]

$$\begin{aligned} \alpha_1 &= (\pi/2)(\delta\mu_0/\lambda)(1/a_1 + 1/b)/\ln(b/a_1) \\ \alpha_2 &= \sqrt{\epsilon_r}(\pi/2)(\delta\mu_0/\lambda)(1/a_2 + 1/b)\ln(b/a_2) \\ &\quad + (2\pi\sqrt{\epsilon_r}/\lambda)\tan\delta \end{aligned} \quad (12)$$

where

$$\begin{aligned} \delta &= \sqrt{2/\omega\mu_0\sigma} \quad \text{skin depth;} \\ \sigma & \quad \text{conductivity of metal;} \\ \tan\delta & \quad \text{loss tangent of dielectric material.} \end{aligned}$$

When $l = \lambda/2$ where λ is a wavelength, and $l_2 = 0$ and there is no shorted end loss, this corresponds to a conventional half-wave resonator. The Q -factor is derived from (14) as follows:

$$Q_0 = 2f_0 W_1 / P_1 = \beta_1 / 2\alpha_1. \quad (13)$$

This is the well-known formula for a conventional half-wave resonator.

III. RESULTS

The numerical calculation was carried out with the following parameters:

frequency	900 MHz;
conductor metal	$\text{Cu } \sigma = 5.8 \times 10^7 (\Omega/m)$
	$r_s = 7.827 \times 10^{-3}$
outer conductor of the resonator	$b = 10 \text{ mm};$
dielectric constant of the ceramics	$\epsilon_r = 35;$
loss tangent of the ceramics	$\tan\delta = 1 \times 10^{-4}.$

The physical dimensions of a PDSIR is designed according to the following resonance condition [1]:

$$\tan\beta_1 l_1 \tan\sqrt{\epsilon_r} \beta_1 l_2 = K \quad (14)$$

where $K = Z_2/Z_1$, and the resonator lengths of line I and II are normalized by a quarter wavelength, that is

$$\begin{aligned} L_1 &= l_1 / \lambda_0 / 4 \\ L_2 &= l_2 / \lambda_0 / 4 \\ L_t &= (l_1 + l_2) / \lambda_0 / 4 \end{aligned} \quad (15)$$

where λ_0 is a wavelength at resonant frequency. In a uniform coaxial resonator of air dielectric, Q -factor has its maximum value at $Z = 77 \Omega$, and this corresponds to $K = 1.0$ and $Z_1 = 77$, $l_1 = \lambda_0/4$, $l_2 = 0$ in a PDSIR. When the Q -factor is normalized, its value is expressed as $Q_n = Q/Q_0$, when Q_0 is given by (13). Where Q_0 also depends on b , and $b = 10 \text{ mm}$ then $Q_0 = 1240$. The

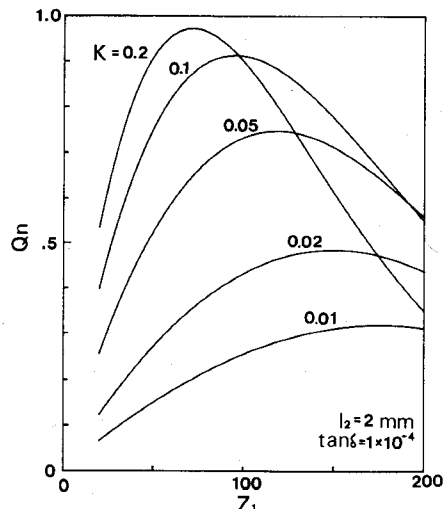
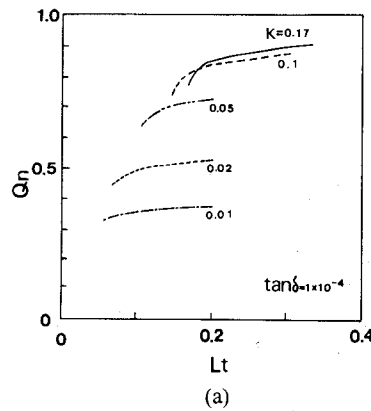
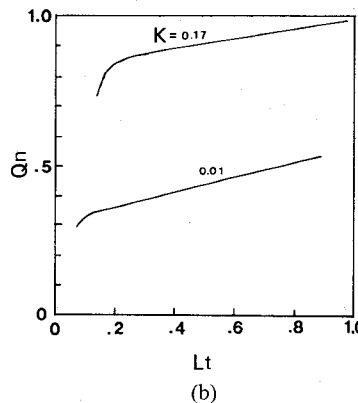


Fig. 2. Normalized Q -factor as a function of Z_1 at various K values with a constant dielectric thickness.



(a)



(b)

Fig. 3. Normalized Q -factor as a function of normalized resonator length L_t .

normalized Q -factor can therefore be expressed by

$$Q_n = Q / 1240 \quad (16)$$

where Q is the calculated value. Fig. 2 shows the Q -factor of a resonator as a function of Z_1 with variable parameter K with the constant dielectric length $l_2 = 2.0 \text{ mm}$. This shows that Z_1 corresponding to a maximum Q increases with decreasing K .

In Fig. 2, the total resonator length also varies with parameter K . When designing a PDSIR, it is important to select K and L_t from the viewpoint of the Q -factor. Fig. 3(a) and (b) shows Q -dependence versus normalized length L_t with different parameter K . Fig. 3(b) illustrates the case with small resonator length

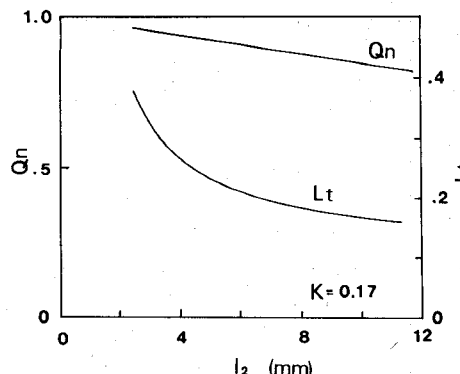


Fig. 4. Normalized Q -factor and normalized resonator length L_t as a function of dielectric thickness at constant K .

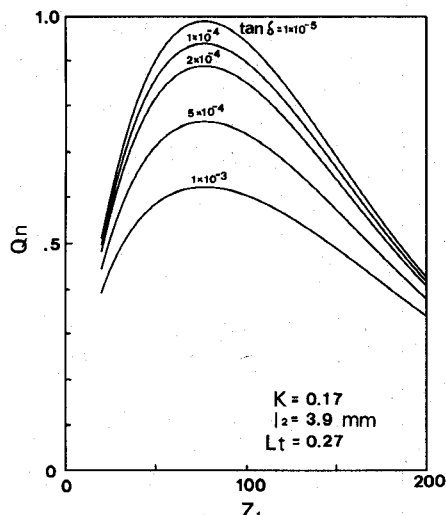


Fig. 5. Normalized Q -factor as a function of Z_1 at various dielectric loss of ceramics.

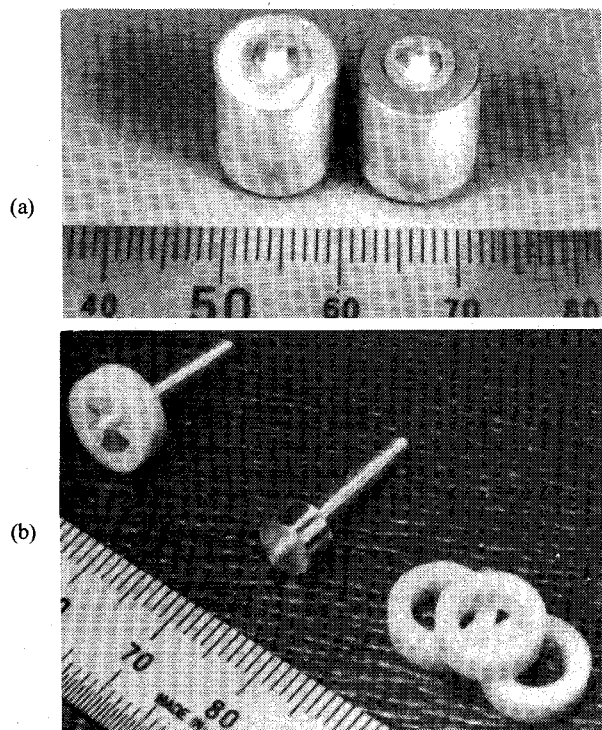


Fig. 6. (a) An experimental PDSIR and (b) an inner conductor with dielectric material.

TABLE I
EXPERIMENTAL AND CALCULATED RESULTS FOR THE Q -FACTOR IN
PDSIR'S AT 900 MHz

No.	Outer conductor diameter b (mm)	Normalized resonator length L_t	Impedance ratio K	Q-factor at 900 MHz	
				Calculated	Experimental
1	15	0.27	0.27	1421	1077
2	15	0.27	0.17	1701	1161
3	10	0.16	1.0	957	773
4	10	0.27	0.2	1004	812
5	10	0.27	0.17	1032	809
6	10	0.15	0.105	868	705
7	10	0.15	0.08	890	729
8	10	0.15	0.06	834	751

and (a) shows the near quarter-wavelength region. As is clearly shown, Q depends greatly on the parameter K and not on resonator length L_t . The Q degradation is small as a function of the resonator length but great when L_t is less than $1/\sqrt{\epsilon_r}$. Fig. 4 shows Q dependence on dielectric length l_2 at constant K . When $K = 0.17$ with $\epsilon_r = 35$, the inner conductor is uniform. Although total resonator length L_t depends greatly on l_2 , Q is only slightly dependent on l_2 . A resonator which is compact in volume can therefore be designed without much Q degradation.

The loss of the dielectric material is also important. The loss factor dependence is shown in Fig. 5 with the same resonator. The Q degradation becomes greater when $\tan \delta$ is larger than 1×10^{-4} .

The experiment was carried out for various resonator lengths and K parameters. Fig. 6 shows the experimental resonator and dielectric ceramics used. A comparison of experimental and calculated Q -factors is shown in Table I. The designed resonant frequency of resonators is not exactly 900 MHz, but the results were all converted to the Q -values of a resonator at 900 MHz.

IV. CONCLUSIONS

The Q -factor of a PDSIR can be analyzed and calculated. From this analysis, the following results are obtained.

- The Q -factor depends greatly on the parameter $K (= Z_2/Z_1)$ rather than the total resonator length L_t .
- The Q -factor degrades greatly when the normalized resonator length $L_t < 0.2$.
- The maximum Q -factor depends on the impedance Z_1 and this becomes high with low K values.

The above results indicate that to obtain a high Q PDSIR, a value for K must be chosen which is as large as possible when the resonator length L_t is small. Such a resonator can be small in size yet have low Q degradation compared with conventional capacitor-loaded resonators.

APPENDIX

The transmission equation in line I including the loss term can be expressed as

$$V(x) = V_0 \cdot \cosh \gamma x = V_0 \cdot \cosh(\alpha_1 + j\beta_1)x$$

$$I(x) = Z_1 \cdot \sinh \gamma x = Z_1 \cdot \sinh(\alpha_1 + j\beta_1)x$$

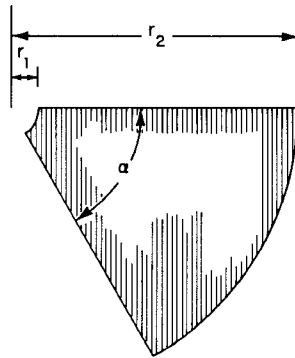
when $\alpha_1 x \ll 1$, $\cosh \alpha_1 x = 1$. Then, V_1 and I_1 at $x = l_1$ can be expressed as (8).

ACKNOWLEDGMENT

The authors are grateful to Dr. S. Kisaka for his continuous encouragement and Y. Aihara for his contribution to the experiments, and Dr. H. Ouchi and S. Kawashima for material development.

REFERENCES

- [1] M. Makimoto and S. Yamashita, "Compact bandpass filters using stepped impedance resonators," *Proc. IEEE*, vol. 67, pp. 16-19, Jan. 1979.
- [2] K. Wakino *et al.*, "Quarter-wave dielectric transmission line duplexer for land mobile communications," in *1979 IEEE MTT-S Int. Microwave Symp. Dig.*, June 1979, pp. 278-280.
- [3] A. Fukasawa *et al.*, "Miniaturized dielectric radio frequency filter for 850-MHz band mobile radio," in *1979 IEEE Vehicular Tech Symp. Dig.*, Mar. 1979, pp. 181-186.
- [4] S. Kawashima *et al.*, "Dielectric properties of $\text{Ba}(\text{Zn}_{1/3}\text{Nb}_{2/3})\text{O}_3$ - $\text{Ba}(\text{Zn}_{1/3}\text{Ta}_{2/3})\text{O}_3$ ceramics at microwave frequency," in *Proc. First Meet. Ferroelectric Appl.*, Apr. 1978, pp. 293-296.
- [5] T. Moreno, *Microwave Transmission Design Data*. New York: Dover, 1948, pp. 62-65.

Fig. 1. Radial-line stub coordinates. (Substrate height = h .)

Microstrip Reactive Circuit Elements

HARRY A. ATWATER, SENIOR MEMBER, IEEE

Abstract—Quantitative design information is given for some planar distributed microwave circuit elements. A microstripline section is calculated as a parallel tuning element, and the radial-line stub and open- and short-circuited coupled microstrip stubs are treated. Typical applications showing measurements on circuits utilizing planar tuning elements are also presented.

I. INTRODUCTION

In the design of microstrip circuits for impedance matching, tuning, and bias-line functions, a relatively limited number of planar circuit configurations is available to fulfill circuit design requirements for inductive, capacitive, and resonant elements. Distributed circuit elements, having dimensions comparable with a wavelength in size, typically require significant amounts of area on the microstrip surface but are simpler to realize in thin film technology than lumped capacitors or inductors.

II. THE RADIAL-LINE STUB

The quarter-wavelength open-ended shunt stub of microstrip line is conventionally employed to establish a point of low impedance relative to the ground plane in mixers and switching circuits and in bias-line circuits. For a stub with low characteristic impedance Z_0 , the point of low impedance at the stub input is indeterminate by an amount equal to the width of the microstripline. A radial-line stub has been proposed to overcome this indeterminacy [1], [2], but a simple calculation for the radii of the resonant radial-line sector (Fig. 1) is not widely available. Based on an assumed radial-wave solution in the substrate dielectric with magnetic walls at the boundary of the stub, Vinding [1] has proposed for the reactance presented at the inner radius r_1

$$X_1 = \frac{h}{2\pi r_1} Z_0(r_1) \frac{360}{\alpha} \frac{\cos(\theta_1 - \psi_2)}{\sin(\psi_1 - \psi_2)} \quad (1)$$

Manuscript received June 6, 1982; revised January 27, 1983. This work was sponsored by the Department of the Army. The views and conclusions contained in this document are those of the contractor and should not be interpreted as necessarily representing the official policies, either expressed or implied, of the United States Government.

The author is with Massachusetts Institute of Technology, Lincoln Laboratory, Lexington, MA 02173.

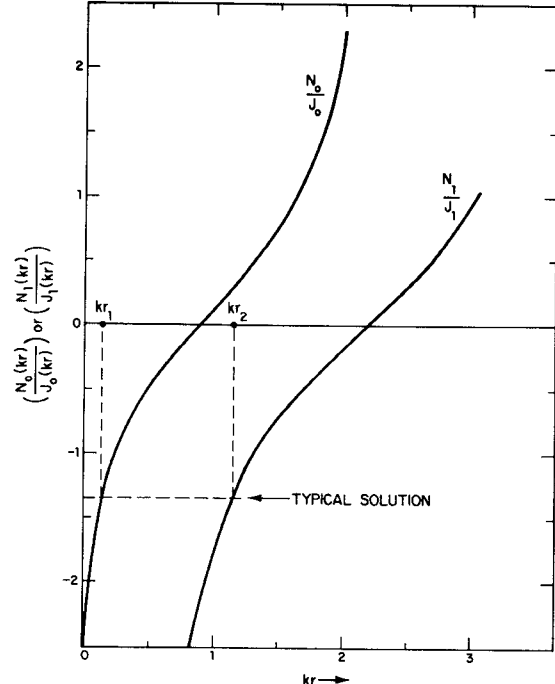


Fig. 2. Plot of (2). Broken line shows typical solution.

where

$$\tan \theta_1 = \frac{N_0(kr_1)}{J_0(kr_1)}$$

$$\tan \psi_i = - \frac{J_1(kr_i)}{N_1(kr_i)} \quad (i = 1, 2)$$

$$Z_0(r_1) = \frac{120\pi}{\sqrt{\epsilon_r}} \left[J_0^2(kr_1) + N_0^2(kr_1) \right]^{1/2} \cdot \left[J_1^2(kr_1) + N_1^2(kr_1) \right]^{-1/2}$$

$$k = 2\pi\sqrt{\epsilon_{re}}/\lambda_0.$$

In (1) above, $J_i(x)$ and $N_i(x)$ are Bessel functions of the first and second kinds, of i th order.

For a resonant stub we assume $X_1 = 0$ in (1), which leads to

$$\frac{N_1(kr_2)}{J_1(kr_2)} = \frac{N_0(kr_1)}{J_0(kr_1)}. \quad (2)$$

A plot of (2) is shown in Fig. 2. A solution of (2) is represented